

---

# Principled change point detection via representation learning

---

**Evgenia Romanenkova \***  
Skoltech

Evgenia.Romanenkova@skoltech.ru

**Alexey Zaytsev**  
Skoltech

a.zaytsev@skoltech.ru

**Ramil Zainulin**  
Skoltech

ramilwm@mail.ru

**Matvey Morozov**  
Skoltech

matvey.morozov@skoltech.ru

## Abstract

Change points are abrupt alterations in the distribution of sequential data. A change-point detection (CPD) model aims at quick detection of such changes. Classic approaches perform poorly for semi-structured sequential data because of the absence of adequate data representation learning. To deal with it, we introduce a principled differentiable loss function that considers the specificity of the CPD task. The theoretical results suggest that this function approximates well classic rigorous solutions. For such loss function, we propose an end-to-end method for the training of deep representation learning CPD models. Our experiments provide evidence that the proposed approach improves baseline results of change point detection for various data types, including real-world videos and image sequences, and improve representations for them.

## 1 Introduction

Modern industry uses complicated systems that continuously work online and are vital for the well-being of large companies and humankind in general. Collapses and prolonged unavailability of such systems lead to significant losses to business owners, so it's important to detect anomalies in their behavior as fast as possible. While potential prone to malicious usage [1], it can greatly benefit the scientific and industrial worlds under reasonable restrictions. A natural way to anomaly detection is to use available historical data for abrupt changes detection. Typically data come from a sequential stream represented as either multivariate vectors from sensors or semi-structured data like videos or event sequences.

Anomaly detection in sequential data actively develops in a framework of machine learning and deep learning. Heuristic approaches include expert-based solutions, adaptations of CNN and GAN methodologies [12, 21, 8, 18]. The majority of methods concentrate on detecting an anomaly in a sequence instead of an accurate *anomaly moment* detection [21, 12]. An alternative approach comes from Change Point Detection (CPD) area: we aim to minimize the delay to disorder detection and the number of false alarms. The CPD problem statement better reflects industrial needs in various scenarios. While in need, examples of using modern deep learning techniques for CPD are scarce if the input data are semi-structured [2].

The challenge here is that the loss functions related to an anomaly detection delay and a number of false alarms are discontinuous. Thus, it is not straightforward to include them in a representation

---

\*This work is supported by the Russian Science Foundation (project 20-71-10135)

learning framework making deep representation learning impossible. So, we need a framework based on representation learning to bridge the gap between industrial and scientific needs and fundamental theory related to change point detection [26].

Our main claims are the following:

- We present a framework for the solution of the CPD problem for semi-structured data. The method detects changes in online mode and makes a decision based on the information available at the current moment.
- To ensure fast and correct change detection, our loss function takes into account both change point detection delay and a number of false change point alarms depicted in Figure 1. It approximates existing loss functions but is continuous and works directly with an intermediate machine learning model.
- Based on this loss function, we propose an end2end framework with a representation learning in the middle. This framework can work with complex semi-structured data structures like multivariate data from sensors, series of images and videos. Our model is based on RNNs to handle the online nature of the problem and the need for a fast model and a typically small amount of available data.
- We provide experiments that can help make a decision, including analysis of change point detection: an ablation study for architectures and hyperparameters of the CPD method, an investigation of an embeddings space, and various metrics for different datasets.

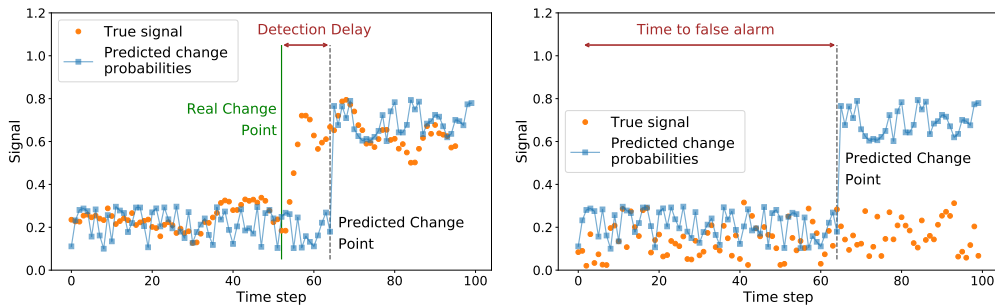


Figure 1: Example of errors during change point detection: delayed change detection (left) and false alarm (right) and corresponding quality metrics Detection Delay and Time to False Alarm. Our approach minimizes a weighted sum of approximations of these loss functions.

## 2 Related work

Change point detection (CPD) and more general Anomaly detection (AD) are widely studied problems in machine learning and statistics for sequential data. Anomaly detection tries to detect if there is an anomaly in a sequence, while the CPD problem focuses on the exact disorder moment. Models and ideas in these areas overlap, so we consider them together below. For more in-depth overview look into review papers and books [22, 4, 26, 2].

**Problem statements** For anomaly or novelty detection, we aim at the detection of a presence of an anomaly for a specific object [19, 14]. For change point detection, we aim at the quickest possible detection of the anomaly or change point moment in a sequence [4]. Change point detection has two typical modes: online and offline. For online change point detection, we signal about a change using only data available at this moment; for offline change point detection, we identify a change point giving a whole sequence of observations. We also classify such problems according to available labels: in some cases, change points are given, and we deal with a supervised change point detection, while in other cases, change point labels are absent, and we consider an unsupervised change point detection. In our paper, we consider *the supervised online change point detection problem*, so we focus on work related to this statement.

**Classic methods** The most classic problem statement consider univariate or small dimension description of a single time moment. In this case, it is proved that statistical methods like CUMSUM [16],

Shiryaev-Roberts [17] and Posterior Probabilities statistics [25] provide a rigorous solution that minimizes delay detection and the number of false alarms given a more specific change point detection problem statement [22]. A general method accumulates these statistics as it runs through a sequence and signals about a change point if the accumulated statistics exceeds a threshold. As in other cases, the theoretical optimality holds under quite strong assumptions and for simple input data. So, there is no direct transfer of the proposed approaches to semi-structured data that urges for intermediate construction of data representations. The review [26] provides a theoretical comparison of various methods advantages distinguishing methods by the cost function, search methods and constraints, but providing no experimental evidence. Another review [2] provides an experimental evaluation of such methods. They conclude that there is no one best approach for detecting changes, so one should carefully select a method considering the specifics of a particular task even for general metrics like accuracy, the area under ROC-curve.

More challenging scenarios that arise in practice with a complex data description often require engineering knowledge to solve. The authors of the paper [3] use ensembles of weak detectors. In [18] the method constructs anomaly score using expert knowledge and basic machine learning approaches. Then it aggregates obtained low-dimensional representations to get anomaly statistics similar to that in [22].

**Representation learning methods** It is tempting to adopt various available neural networks solutions to the CPD problem. A straightforward approach is given in [9]. The authors provide evidence that for various univariate and multivariate datasets, it is possible to detect change points via a simple neural network. However, they don't consider semi-structured sequential data and generate change probabilities using a single element of sequences. Thus, it is impossible to apply their approach to sequential data with complex dynamics. A natural improvement is to use recurrent neural network architectures [7, 10] for change point and anomaly detection [15, 6]. It provides high-quality models in supervised problems and can be used for various data types. More sophisticated models can take advantage of unlabeled data and adopt GAN ideas. The main difficulty for such models is taking into account the temporal component in a generative model. The paper [27] introduces a TimeGAN model capable of time series generation regarding the original relationships between variables across time. They show that although TimeGAN improves over many state-of-the-art benchmarks, the results aren't significantly different from the RNN-based GAN.

Change point detection can also be considered as an example of a more general task, Anomaly Detection in Time Series. In [13, 8], the authors use LSTM as a prediction model and then compute the prediction error distribution. The resulting prediction errors are modelled as a multivariate Gaussian distribution. Therefore, the observation is an anomaly if they appear in the tails of this distribution. The paper [21] suggests a particular end-to-end method for anomaly detection based on neural networks. Based on a well-known approach for anomaly detection SVDD, the authors offer the improvement that took into account temporal dynamics of data. In [12], the authors proposed a GAN-based Anomaly Detection (GAN-AD) method for Cyber-Physical Systems (CPSs). To deal with sequential data, they use LSTM for both generator and discriminator. Then they use the classical approach for anomaly detection provided by GAN: a combination of discriminator loss and difference between the reconstructed testing samples and the actual testing samples. The authors also ignore precise change moment detection, focusing on general anomaly detection.

**Conclusions** Thus, the current state of the art shows that it is possible to construct neural-networks based solutions for anomaly detection. At the same time, they can't identify precise change moments crucial for many applications. On the other hand, a more theoretical area is related to change detection, but with too restrictive assumptions and limited ability to learn complex data representation. In our work, we tried to bridge this gap and proposed a principled solution for representation learning devoted to a change point detection problem. As the amount of available data in such a problem is moderate, we'll focus on neural networks architectures with smaller number parameters like LSTMs and GRUs while critically examining our design choices.

### 3 Methods

#### 3.1 Change point detection

We consider a realization of a random process  $X^{1:T} = \{\mathbf{x}_1, \dots, \mathbf{x}_T\}$  of length  $T$ . Each element  $\mathbf{x}_i \in \mathbb{R}^d$  corresponds to an observation at time  $i$ . The process depends on the latent variable  $\theta \in \{0, 1, \dots, \infty\}$ . For  $\theta = \infty$ , the data always come from a distribution  $f_\infty$ . For  $\theta = 0$ , the data always come from a distribution  $f_0$ . More interesting are in-between cases, when for  $t < \theta$  the process' behaviour is normal, and the data come from  $f_\infty$ , and for  $t \geq \theta$  — abnormal with the distribution  $f_0$ . We assume that  $\theta$  follows the distribution  $\mathbb{G}$ . The problem is the quickest detection of the true change moment  $\theta$  using an as small amount of data  $X^{1:T'}$ ,  $T' \leq T$  as possible.

Following [22], we are looking for an optimal change point  $\tau^*$  such that:

$$\tau^* = \arg \inf_{\tau \in \mathfrak{M}_a} \mathbb{E}_{\mathbb{G}}(\tau - \theta)^+, \text{ where } \mathfrak{M}_a = \{\tau : \mathbb{E}_0 \tau \geq a\},$$

$\mathbb{E}_0$  is the expectation given that there are no change point in a sequence, so the minimization of  $\mathbb{E}_{\mathbb{G}}(\tau - \theta)^+$  specifies that we want low value for detection delay  $(\tau - \theta)^+$ .  $\mathfrak{M}_a$  states, that we are looking only for procedures with Average Time to False alarm larger than  $a$ .

Using the method of Lagrange multipliers with parameter  $c$ , we rewrite (1) as a single loss that consists of two terms:

$$\tau^* = \arg \inf_{\tau} L(\tau), \text{ where } L(\tau) = \mathbb{E}_{\mathbb{G}}(\tau - \theta)^+ - c \mathbb{E}_0 \tau. \quad (1)$$

#### 3.2 Loss function approximation

A dataset is a set of sequences  $D = \{(X_1, \theta_1), \dots, (X_N, \theta_N)\}$ , where each sequence  $X_i$  has the length  $T$  and corresponding change point  $\theta$  is in  $[1, \dots, T]$ , if we have a change point in a sequence and  $\theta = (T + 1)$  otherwise. A model  $f_{\mathbf{w}}$  produce series of outputs  $\mathbf{p}_i = \{p_{ti}\}$  for  $t \in \{1, \dots, T\}$  that correspond to the probabilities  $p_{ti} = f_{\mathbf{w}}(X_i^{1:t})$  of the change point at a specified time moment  $t$ . The model output  $f_{\mathbf{w}}(X_i^{1:t})$  at the moment  $t$  depends only on the information available up to this moment  $X_i^{1:t}$ . Formally, we detect a change point at a point  $t$  with probability  $p_{ti}$ , if we didn't report about a change point before. Our goal is to construct a model  $f_{\mathbf{w}}(X_i^{1:t})$  with the smallest loss value (1).

Inspired by the method above, we suggested a new principled loss function to train a neural network model  $f_{\mathbf{w}}$ . The expected value of detection delay  $\mathcal{L}_{delay}$  given the probabilities has the following form:

$$\mathcal{L}_{delay}(f_{\mathbf{w}}, D) = \frac{1}{N} \sum_{i=1}^N \left( \sum_{t=\theta}^{\infty} (t - \theta_i) p_{ti} \prod_{k=\theta_i}^{t-1} (1 - p_{ki}) \right), \quad (2)$$

the outer sum over  $i$ -s reflects that we average the loss over all sequences with a change point in a batch, the inner sum over  $t$ -s correspond to losses associated with each moment in a sequence. The expected time to false alarm  $\mathcal{L}_{FA}$  given the probabilities has the following form:

$$\mathcal{L}_{FA}(f_{\mathbf{w}}, D) = N - \frac{1}{N} \sum_{i=1}^N \left( \sum_{t=0}^{\theta_i} (t - \theta_i) p_{ti} \prod_{k=0}^{\theta_i} (1 - p_{ki}) \right). \quad (3)$$

The final loss, that corresponds to (1), is a weighted sum of  $\mathcal{L}_{delay}(f_{\mathbf{w}}, D)$  and  $\mathcal{L}_{FA}(f_{\mathbf{w}}, D)$  defined by the coefficient  $c$ :

$$\mathcal{L}(f_{\mathbf{w}}, D) = \mathcal{L}_{delay}(f_{\mathbf{w}}, D) + c \mathcal{L}_{FA}(f_{\mathbf{w}}, D). \quad (4)$$

It is easy to see that this loss function is differentiable with respect to model outputs  $p_i$ . Thus, it can be optimized by a neural network to train the mapping from initial data  $X_{1:k}$  to  $p_k$  that minimizes the loss function.

As it can be seen, the loss 2 depends on the real change moment  $\theta$ . As a result, there will be a different number of terms in the sum for different inputs. To deal with it, we propose the following approximation for  $\mathcal{L}_{delay}$ :

$$\tilde{\mathcal{L}}_{delay}(f_{\mathbf{w}}, D) = \frac{1}{N} \sum_{i=1}^N \left( \sum_{t=\theta_i}^T (t - \theta_i) p_{ti} \prod_{k=\theta_i}^{t-1} (1 - p_{ki}) + (T + 1 - \theta_i) \prod_{k=\theta_i}^T (1 - p_{ki}) \right), \quad (5)$$

where  $T$  — some hyperparameter restricted by the size of a considered segment.

So, our final loss function is:

$$\tilde{\mathcal{L}}(f_{\mathbf{w}}, D) = \tilde{\mathcal{L}}_{delay}(f_{\mathbf{w}}, D) + c \mathcal{L}_{FA}(f_{\mathbf{w}}, D). \quad (6)$$

**Theorem 3.1.** *The loss function  $\tilde{\mathcal{L}}(f_{\mathbf{w}}, D)$  from (6) is a lower bound for  $L(\tau)$  from criteria (1).*

The proof is given in Appendix. So, given the results above, our differentiable loss function is a lower bound for a principled loss function in (1). We expect that the proposed loss is an accurate approximation to the true one since the high terms in the sums are negligible because for the most applied problems, we end up detecting change sooner or later base on data from a sequence.

### 3.3 End-to-end change point detection

The resulting training pipeline given a dataset  $D = \{X_i\}_{i=1}^N$  is the following:

1. Get change point probabilities  $\mathbf{p}_k$  using a neural network  $f_{\mathbf{w}}(X_k)$  for  $k = \overline{1, N}$ ;
2. Calculate a differentiable loss function  $L(f_{\mathbf{w}}, D)$ ;
3. Evaluate the loss function derivatives to update the neural network parameters  $\mathbf{w}$ .

In our approach we use *Custom*  $\tilde{\mathcal{L}}(f_{\mathbf{w}}, D)$  (6) loss. As an alternative to the network trained with our loss  $\mathcal{L}$ , we consider a baseline. A binary classification problem can approximate our CPD problem: we classify each time moment as either a moment before or after the change to get the change point probabilities  $p_i$ . To train a model that predicts these probabilities, we use the binary cross-entropy loss *BCE* for predictions and true sequence labels. We also *combine* them by training the model several epochs with *BCE* loss and then by training it with *Custom* loss.

## 4 Experiments

In this section, we demonstrate how our change-point detection approach works in real-data scenarios. The main results are given for all datasets, while due to space limitations, we demonstrate more specific results only via one dataset, as for other datasets, results were almost similar in our experiments. The code is published online<sup>2</sup>.

### 4.1 Comparison details

We compare three possible options in our computational experiments: binary cross entropy loss (BCE), our loss (Custom), and a combination of BCE and Custom losses (Combined). We train a neural network with a selected architecture with no other changes for specific loss functions above. For different datasets and data types, we adopt best practices for the selection of hyperparameters. Implementation details are given in Appendix.

### 4.2 Datasets

We use sequential data with various complexity: from synthetic sequences and multivariate data from sensors to video datasets. Detailed information on datasets and their preprocessing are given in Appendix.

<sup>2</sup>The code is available at <https://anonymous.4open.science/r/CPD>

Table 1: Main quality metrics for considered loss functions.  $\uparrow$  marks metrics we want to maximize,  $\downarrow$  marks metrics we want to minimize.

Loss	Mean Time to FP	Mean delay $\downarrow$	TP $\uparrow$	FP $\downarrow$	F1 score $\uparrow$	Area under detec. curve $\downarrow$
Normal Distribution 1d						
BCE	95	0.040	43	4	0.956	1017.94
	99	1.380	44	<b>0</b>	0.978	
Custom (ours)	95	<b>0.010</b>	<b>45</b>	6	0.938	980.03
	99	1.080	44	<b>0</b>	0.978	
Combined (ours)	95	0.080	<b>45</b>	11	0.891	<b>978.12</b>
	99	0.840	<b>45</b>	<b>0</b>	<b>0.989</b>	
Multivariate Normal Distribution 100d						
BCE	60	<b>0.010</b>	<b>93</b>	7	<b>0.964</b>	2750.91
	75	30.470	87	<b>0</b>	0.930	
Custom (ours)	60	3.660	59	35	0.742	<b>2121.80</b>
	75	10.590	84	<b>0</b>	0.913	
Combined (ours)	60	0.930	92	7	0.958	2607.56
	75	14.610	83	<b>0</b>	0.907	
Human Activity						
BCE	10	1.438	19	13	0.745	69.32
	11	3.594	<b>26</b>	<b>4</b>	<b>0.897</b>	
Custom (ours)	10	<b>0.406</b>	7	25	0.359	59.06
	11	0.594	10	22	0.476	
Combined (ours)	10	0.688	15	17	0.638	<b>55.36</b>
	11	0.906	15	17	0.638	
MNIST						
BCE	44	0.938	60	37	0.534	477.40
	48	35.167	20	<b>0</b>	0.345	
Custom (ours)	44	1.115	35	61	0.534	<b>392.01</b>
	48	9.021	40	33	0.588	
Combined (ours)	44	<b>0.729</b>	50	48	0.676	516.84
	48	20.583	<b>74</b>	<b>0</b>	<b>0.871</b>	
Explosion						
BCE	13	0.670	8	11	0.471	5.40
	15	0.989	8	4	0.533	
Custom (ours)	13	<b>0.352</b>	8	21	0.372	4.35
	15	1.193	9	2	<b>0.581</b>	
Combined (ours)	13	0.625	<b>10</b>	18	0.465	<b>4.12</b>
	15	0.716	8	<b>1</b>	0.533	
OOPS						
BCE	6	<b>0.027</b>	5	<b>1</b>	0.011	20.23
	8	2.734	0	309	0.000	
Custom (ours)	6	0.352	118	2	0.236	15.02
	8	0.731	<b>153</b>	15	<b>0.303</b>	
Combined (ours)	6	0.036	45	<b>1</b>	0.097	<b>14.97</b>
	8	0.166	68	5	0.144	

**Synthetic sequences.** We start with two toy examples: 1D and 100D Gaussians with a change in the mean of the distribution and without it.

**Human Activity Dataset.** As a dataset with numerical sequences, we use the USC-HAD dataset [28] with 12 types of human activity. These sequences are cutted, so that there are sequences with change in the type of human activity and without change. Each sequence consists of measurements of 561 features during 20 time ticks.

**Sequences of MNIST images.** We generate another dataset on the base of MNIST [11] images. With a Conditional Variational Autoencoder (CVAE) [23] we construct sequences with and without change. Sequences with a change start and end with two images from similar classes that smoothly

transform one into another. Sequences with a change start and end with two images from different classes. We generated a balanced dataset of 1000 sequences with length 64.

**Explosions.** UCF-Crime is a video dataset for anomaly detection for sequences [24]. It consists of real-world 240x320 videos, with 13 realistic anomaly types such as explosion, road accident, burglary, etc., and normal examples. Among all video types we consider only explosions, as they correspond not to a point anomaly, but to a distribution change. Each sequences length after preprocessing was 16.

**Unintentional actions.** OOPS dataset includes 20338 fail compilation videos. Each one consists of two parts: an intentional action before the fail *point of change* and an unintentional one after [5]. We use 1000 videos for the training set and 500 videos for the test set for our purpose. Each video has 16 frames and FPS 8.

### 4.3 Benchmarks and Metrics

**Classification quality metrics.** For our problem statement, elements of the confusion matrix have the following meaning. For True Positive (TP), we correctly detect changes no earlier than it appears. We report False Positive (FP) if a model predicts a change in a normal sequence or before an actual disorder.

**Delay detection and Time to False Alarm.** For a quantitative comparison of CPD approaches, we concentrate on typical metrics for change point detection: Delay Detection and Time to False Alarm depicted in Figure 1. We want to meet two competing goals: minimize the Detection Delay and maximize the Time to False Alarm. The Delay Detection  $(\tau - \theta)^+$  is the difference between the true change point  $\theta$  and the model’s prediction of change point  $\tau$ . The Time to False Alarm  $\tau$  is the difference between a first false positive prediction if it exists and the sequence start.

**Area under the detection curve.** We report as the change the first time when the model change probability prediction  $p_t$  exceed a threshold  $s$ . Varying  $s$ , we obtain different trade-offs between mean detection delay and mean time to a false alarm. To overview all possible options, we propose to measure the area under the curve obtained via varying the change detection threshold  $s$ . We want to find an approach that minimises the area under such curve for  $x$ -axis Mean Time to False Alarm and  $y$ -axis Mean Detection Delay time. As this metric provides an overall performance evaluation, we consider it as the main quality metric for comparing our approaches.

### 4.4 Main results

Table 1 presents metrics for various datasets. We consider the most important values for mean time to False Alarms. It can be seen that our proposed methods outperform the baseline in terms of main metrics Delay Detection and Time to False Alarms while having lower common classification metrics. We suppose that such behaviour is caused by a higher number of True Positives for BCE loss while higher detection delay. So, the model detects a change point with a significant gap.

We continue with Figure 2 on how threshold selection affects quality metrics for considered change detection approaches. For 1D synthetic cases, the performances of all models are similar due to the simple structure of the data. Our principled loss function provides performance improvements over BCE loss. The results for 100D synthetic sequences are ambiguous. Although the BCE has lower mean delay detection for some thresholds, the results area under the curve is lower for proposed methods. For more complex data such as MNIST sequences and video datasets, the models with Custom loss always defeats the models with BCE loss. As for Combined loss, its results in the case of the MNIST dataset are similar to BCE, while they are similar to the Custom loss for videos.

### 4.5 Result analysis

We also investigate the probabilities given by the models for different loss functions. Figure 3 shows histogram for predictions on Explosion dataset. It can be seen that model with BCE loss outputs probabilities lower than a model with Custom or Combined losses after a change point. Thus, we suppose that using our loss helps the network to change probabilities sharper. Figure 4 also supports this hypothesis. The probabilities provided by using the BCE model after a disorder in the data. For example, for the case from the left picture in 4, the BCE model doesn’t detect any changes for low threshold.

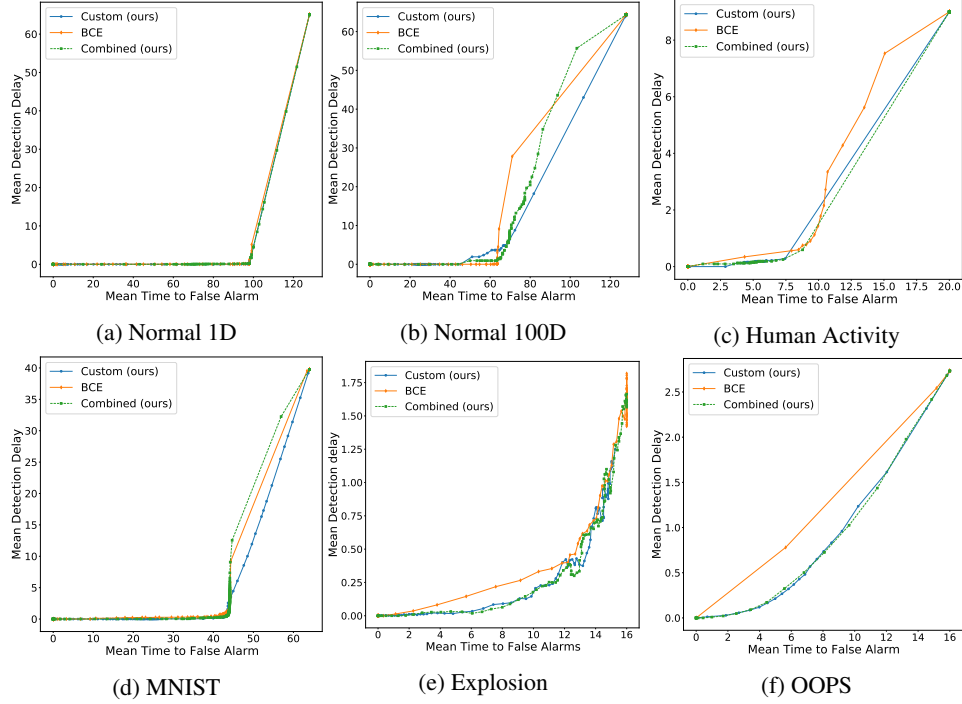


Figure 2: The performance detection curves for various datasets. We train models with Custom, BCE and Combined loss calculate metrics for a different threshold for each dataset. The models trained with our losses have better results on all type of data except very simple case (a) where performance is similar.

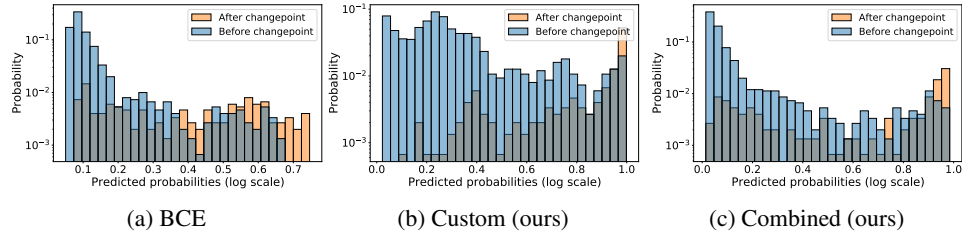


Figure 3: Histograms of model predictions for Explosion dataset. The model trained with BCE loss has lower probabilities which denote uncertainty about predictions.

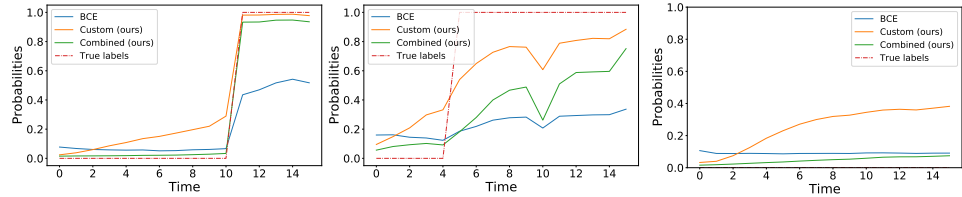


Figure 4: Typical examples with change point (left, center) and without (right) of model predictions for Explosion dataset.

To check the quality of obtained representations, we present tSNE embeddings for them in Figure 5. We show embeddings for MNIST data before, immediately after a change occurs and later. The model trained with BCE loss doesn't bother about fast change. Embeddings for points immediately after the change are close to that before the change. Thus, we'll have a significant detection delay. For our loss, embeddings for figures after change rapidly move to a separate region, making change point detection faster and more accurate. For the combined model, the embeddings after change lie



even farther. Moreover, we guess that the third class, which appeared in tSNE for Combined loss, corresponds to sequences' transition moment (when a number smoothly changes to another). Using Combined loss improve representations in such areas compared to the Custom loss.

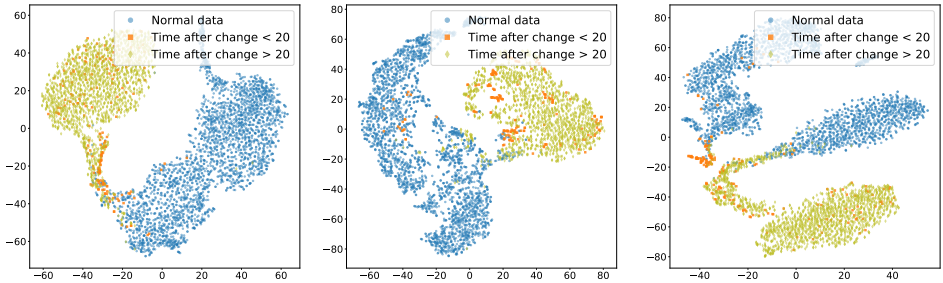


Figure 5: tSNE for embeddings obtained via approaches with the binary cross-entropy loss (left), and our custom loss (center), and our combined loss (right).

#### 4.6 Ablation study

We examine various design choice to see how they affect the model performance. For our loss (6) we can select the contribution of terms related to detection delay and false alarms. We balance them by the selection of the coefficient  $a$ , such that  $\mathcal{L}(f_w, D) = a \cdot \mathcal{L}_{delay}(f_w, D) + (1 - a) \cdot \mathcal{L}_{FA}(f_w, D)$ . As we see on the left in Figure 6 the reasonable choice of the weight,  $a$  only moderately affects the performance. As we see on the right in Figure 6 our approximation is pretty accurate, and we don't need a large number of components in it. On the other hand, the inclusion of a larger number of components doesn't harm the numerical stability of our approach.

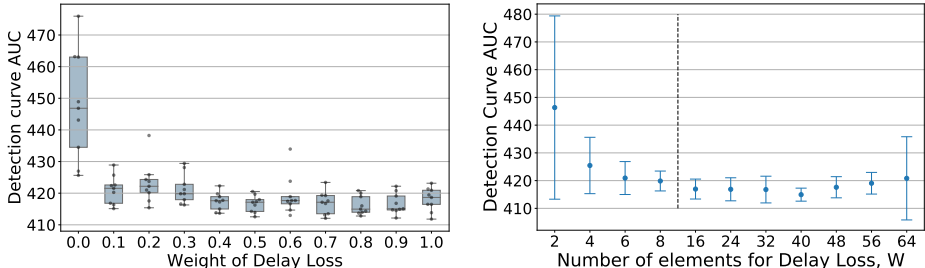


Figure 6: The model's performance dependence from weights for False Alarm and Detection delay loss component(left) and number of elements for Delay Loss (right) for MNIST data for Custom loss averaged over 10 runs. If we have both components of loss, we produce a pretty stable result. If we include about 16 or more elements in our loss, we obtain reasonable results.

## 5 Conclusions

We proposed a principled loss function that allows quick change detection with a low number of false alarms for semi-structured sequential data. Our loss function is a differentiable lower bound for a loss function from the fundamental CPD literature. Thus, it allows end2end training of neural networks models for representation learning and quality metrics at hand. Our approach provides benefits in various scenarios, including the processing of data from sensors and video stream.

## References

- [1] J. R. Agustina and G. G. Clavell. The impact of cctv on fundamental rights and crime prevention strategies: The case of the catalan control commission of video surveillance devices. *Computer law & security review*, 27(2):168–174, 2011.
- [2] S. Aminikhangahi and D. J. Cook. A survey of methods for time series change point detection. *Knowledge and information systems*, 51(2):339–367, 2017.

- [3] A. Artemov and E. Burnaev. Detecting performance degradation of software-intensive systems in the presence of trends and long-range dependence. In *2016 IEEE 16th International Conference on Data Mining Workshops (ICDMW)*, pages 29–36. IEEE, 2016.
- [4] M. Basseville, I. V. Nikiforov, et al. *Detection of abrupt changes: theory and application*, volume 104. Prentice hall Englewood Cliffs, 1993.
- [5] D. Epstein, B. Chen, and C. Vondrick. Oops! predicting unintentional action in video. In *Proceedings of the IEEE/CVF conference on computer vision and pattern recognition*, pages 919–929, 2020.
- [6] T. Figliolia and A. G. Andreou. An fpga multiprocessor architecture for bayesian online change point detection using stochastic computation. *Microprocessors and Microsystems*, 74:102968, 2020.
- [7] K. Greff, R. K. Srivastava, J. Koutník, B. R. Steunebrink, and J. Schmidhuber. Lstm: A search space odyssey. *IEEE transactions on neural networks and learning systems*, 28(10):2222–2232, 2016.
- [8] K. Hundman, V. Constantinou, C. Laporte, I. Colwell, and T. Soderstrom. Detecting spacecraft anomalies using lstms and nonparametric dynamic thresholding. In *Proceedings of the 24th ACM SIGKDD international conference on knowledge discovery & data mining*, pages 387–395, 2018.
- [9] M. Hushchyn, K. Arzumatov, and D. Derkach. Online neural networks for change-point detection. *arXiv preprint arXiv:2010.01388*, 2020.
- [10] R. Jozefowicz, W. Zaremba, and I. Sutskever. An empirical exploration of recurrent network architectures. In *International conference on machine learning*, pages 2342–2350. PMLR, 2015.
- [11] Y. LeCun and C. Cortes. MNIST handwritten digit database. 2010. URL <http://yann.lecun.com/exdb/mnist/>.
- [12] D. Li, D. Chen, J. Goh, and S.-k. Ng. Anomaly detection with generative adversarial networks for multivariate time series. *arXiv preprint arXiv:1809.04758*, 2018.
- [13] P. Malhotra, L. Vig, G. Shroff, and P. Agarwal. Long short term memory networks for anomaly detection in time series. In *Proceedings*, volume 89, pages 89–94. Presses universitaires de Louvain, 2015.
- [14] M. Markou and S. Singh. Novelty detection: a review—part 1: statistical approaches. *Signal processing*, 83(12):2481–2497, 2003.
- [15] F. J. Ordóñez and D. Roggen. Deep convolutional and LSTM recurrent neural networks for multimodal wearable activity recognition. *Sensors*, 16(1):115, 2016.
- [16] E. S. Page. Continuous inspection schemes. *Biometrika*, 41(1/2):100–115, 1954.
- [17] M. Pollak and A. G. Tartakovsky. Optimality properties of the shiryayev-roberts procedure. *Statistica Sinica*, pages 1729–1739, 2009.
- [18] E. Romanenkova, A. Zaytsev, N. Klyuchnikov, A. Gruzdev, K. Antipova, L. Ismailova, E. Burnaev, A. Semenikhin, V. Koryabkin, I. Simon, et al. Real-time data-driven detection of the rock-type alteration during a directional drilling. *IEEE Geoscience and Remote Sensing Letters*, 17(11):1861–1865, 2019.
- [19] L. Ruff, J. R. Kauffmann, R. A. Vandermeulen, G. Montavon, W. Samek, M. Kloft, T. G. Dietterich, and K.-R. Müller. A unifying review of deep and shallow anomaly detection. *Proceedings of the IEEE*, 2021.
- [20] M. Sandler, A. Howard, M. Zhu, A. Zhmoginov, and L.-C. Chen. Mobilenetv2: Inverted residuals and linear bottlenecks. In *Proceedings of the IEEE conference on computer vision and pattern recognition*, pages 4510–4520, 2018.
- [21] L. Shen, Z. Li, and J. Kwok. Timeseries anomaly detection using temporal hierarchical one-class network. *Advances in Neural Information Processing Systems*, 33:13016–13026, 2020.
- [22] A. Shiryaev. Stochastic change-point detection problems. *Moscow: MCCME (in Russian)*, 2017.
- [23] K. Sohn, H. Lee, and X. Yan. Learning structured output representation using deep conditional generative models. *Advances in neural information processing systems*, 28:3483–3491, 2015.

- [24] W. Sultani, C. Chen, and M. Shah. Real-world anomaly detection in surveillance videos. In *Proceedings of the IEEE conference on computer vision and pattern recognition*, pages 6479–6488, 2018.
- [25] A. G. Tartakovsky and G. V. Moustakides. State-of-the-art in bayesian changepoint detection. *Sequential Analysis*, 29(2):125–145, 2010.
- [26] C. Truong, L. Oudre, and N. Vayatis. Selective review of offline change point detection methods. *Signal Processing*, 167:107299, 2020.
- [27] J. Yoon, D. Jarrett, and M. van der Schaar. Time-series generative adversarial networks. 2019.
- [28] M. Zhang and A. A. Sawchuk. USC-HAD: a daily activity dataset for ubiquitous activity recognition using wearable sensors. In *Proceedings of the 2012 ACM Conference on Ubiquitous Computing*, pages 1036–1043, 2012.

## Checklist

1. For all authors...
  - (a) Do the main claims made in the abstract and introduction accurately reflect the paper’s contributions and scope? [\[Yes\]](#)
  - (b) Did you describe the limitations of your work? [\[Yes\]](#) See discussions in Section 4.
  - (c) Did you discuss any potential negative societal impacts of your work? [\[Yes\]](#) See Section 1.
  - (d) Have you read the ethics review guidelines and ensured that your paper conforms to them? [\[Yes\]](#)
2. If you are including theoretical results...
  - (a) Did you state the full set of assumptions of all theoretical results? [\[Yes\]](#) In Section 3.
  - (b) Did you include complete proofs of all theoretical results? [\[Yes\]](#) In Section 3.
3. If you ran experiments...
  - (a) Did you include the code, data, and instructions needed to reproduce the main experimental results (either in the supplemental material or as a URL)? [\[Yes\]](#) We provide link for the code to run the experiments
  - (b) Did you specify all the training details (e.g., data splits, hyperparameters, how they were chosen)? [\[Yes\]](#) We provide data processing in Section 4. We provide training details partly in the main part of the article, partly in Appendix.
  - (c) Did you report error bars (e.g., with respect to the random seed after running experiments multiple times)? [\[Yes\]](#) We provide results of an average of multiple runs and reflect this in the paper for most crucial in Section 4 w.
  - (d) Did you include the total amount of compute and the type of resources used (e.g., type of GPUs, internal cluster, or cloud provider)? [\[N/A\]](#) Not relevant because the focus of the work is different, and all considered methods use a similar amount of computational resources.
4. If you are using existing assets (e.g., code, data, models) or curating/releasing new assets...
  - (a) If your work uses existing assets, did you cite the creators? [\[Yes\]](#)
  - (b) Did you mention the license of the assets? [\[Yes\]](#) if required
  - (c) Did you include any new assets either in the supplemental material or as a URL? [\[Yes\]](#) We provide code for the generation of new artificial data or data based on existing real datasets
  - (d) Did you discuss whether and how consent was obtained from people whose data you’re using/curating? [\[N/A\]](#)
  - (e) Did you discuss whether the data you are using/curating contains personally identifiable information or offensive content? [\[N/A\]](#)
5. If you used crowdsourcing or conducted research with human subjects...
  - (a) Did you include the full text of instructions given to participants and screenshots, if applicable? [\[N/A\]](#)

- (b) Did you describe any potential participant risks, with links to Institutional Review Board (IRB) approvals, if applicable? [N/A]
- (c) Did you include the estimated hourly wage paid to participants and the total amount spent on participant compensation? [N/A]

## A Appendix

The supplementary materials contain proofs of suggested theorems in Section A.1, details about data preprocessing and data examples in Section A.2, implementation details in Section A.3, and an extended table with additional quality metrics in Section A.4.

### A.1 Proofs

We provide here proof that our loss function is a lower bound of the principled loss function. We start with a supplementary lemma, then continue with the main theorem.

**Lemma A.1.**  $\tilde{\mathcal{L}}_{delay}(f_{\mathbf{w}}, D)$  is a lower bound for  $\mathcal{L}_{delay}(f_{\mathbf{w}}, D)$ .

*Proof.* Rewrite  $\mathcal{L}_{delay}(f_{\mathbf{w}}, D)$  in the following form:

$$\mathcal{L}_{delay}(f_{\mathbf{w}}, D) = \frac{1}{N} \sum_{i=1}^N \left( \sum_{t=\theta_i}^T (t - \theta_i) p_{ti} \prod_{k=\theta}^{t-1} (1 - p_{ki}) + \sum_{t=T+1}^{\infty} (t - \theta_i) p_{ti} \prod_{k=\theta_i}^{t-1} (1 - p_{ki}) \right)$$

for some T. Consider the second term for a single sequence:

$$\sum_{t=T+1}^{\infty} (t - \theta) p_t \prod_{k=\theta}^{t-1} (1 - p_k) \geq (T + 1 - \theta) \sum_{t=T+1}^{\infty} p_t \prod_{k=\theta}^{t-1} (1 - p_k).$$

At the same time, the expression under the sum introduces the probability of detecting the change moment somewhere after the moment  $T + 1$ . It equals to the probability of not detecting the change before moment  $T + 1$ . Thus,

$$(T + 1 - \theta) \sum_{t=T+1}^{\infty} p_t \prod_{k=\theta}^{t-1} (1 - p_k) = (T + 1 - \theta) \prod_{t=\theta}^T (1 - p_t).$$

This brings us to the desired result.  $\square$

**Theorem A.1.** The loss function  $\tilde{\mathcal{L}}(f_{\mathbf{w}}, D)$  from (4) is a lower bound for  $L(\tau)$  from criteria (1).

*Proof.* Let us define  $\mathcal{L}_{delay_t} = (t - \theta) p_t \prod_{k=\theta}^{t-1} (1 - p_k)$ . Then  $\sum_{t=\theta}^{\infty} \mathcal{L}_{delay_t}$  corresponds to the detection delay for a single sequence. If we detect the change moment perfectly, then the delay equals 0 and  $\mathcal{L}_{delay_0} = 0$ . For time  $t$ , the actual delay will be equal to the difference between the moment of detection  $t$  and the real moment  $\theta$ .

To calculate the delay expectation  $\mathbb{E}(\tau - \theta)^+$ , we must consider the probability of detecting a fault at time  $t$  and not detecting it for all previous moments  $\{\theta, \dots, t - 1\}$ . Thus,  $\mathcal{L}_{delay_t} = (t - \theta) p_t \prod_{k=\theta}^{t-1} (1 - p_k)$ .

By summation of  $\mathcal{L}_t$  for all  $t = \{\theta, \dots, \infty\}$  and averaging over all sequences, we get (2) that is then equal to  $\mathbb{E}_{\mathbb{G}}(\tau - \theta)^+$ .

Applying A.1, we get that the first term in (4) is a lower bound for  $\mathbb{E}_{\mathbb{G}}(\tau - \theta)^+$ .

Similarly, we consider the second term in (4). The first difference is that we should count the moments before the actual moment of change. The second significant difference is that we want to maximize time to false positive, so we should add a minus sign. Finally, we lower bounded two terms in  $L(\tau)$  by two terms in  $\tilde{\mathcal{L}}(f_{\mathbf{w}}, D)$ .  $\square$

### A.2 Datasets details

In the paper, we consider a diverse set of datasets. Summary statistics on the data used are shown in the Table 2. More information about data generation and preprocessing are provided below.

**Synthetic datasets.** The first part of a sequence in this dataset corresponds to the "normal" state and sampled from  $\mathcal{N}(1, 1)$  in one-dimensional case, and  $\mathcal{N}(\mathbf{1}, I)$  in multi-dimensional case, where  $\mathbf{1} -$

array of shape 100 filled with ones and  $I$  is an identity matrix of size 100. As a change, we sampled vectors from a normal distribution with a randomly selected mean between 3 and 100 and the same variance as in the normal case. We want to test our approach in the cases when there are either sequences with changes in the training set or not. Thus, we do not add sequences without changes in the 100D case, while in the 1D case, the number of such sequences equals half of the whole set.

**Human Activity dataset** contain sensors’ records for 12 types of human physical activity, such as walking, elevator, going upstairs, running, sleeping, etc. collected from the group of 30 individuals. Each record has a length of 200 and consists of 561 features. The frequency of sensor measurements is 50 Hz. We cut these sequences so that there are sequences with change in the type of human activity. The result length of every subsequence is 20.

**Sequences of MNIST images.** To generate data, we obtain a latent representation for MNIST images by using Conditional Variational Autoencoder [23] (CVAE). Then we take two points corresponding to a certain pair of digits and also add the points from the line connecting two initial points. As a result, we have a sequence of latent representations of images. After reconstruction via CVAE, we get a sequence of images. Such an approach allows us to generate images that change continuously, even if there is a change in a digit. There are sequences with (e.g. from 4 to 7) and without (e.g. from 4 to 4) a change point in the result dataset. We generate 1000 sequences with length 64 distributed evenly between normal and sequences with changes for our experiment. Two examples of obtained sequences are in Figure 7.

**Explosion.** It consists of real-world  $240 \times 320$  RGB videos, with 13 realistic anomaly types such as explosion, road accident, burglary, etc., and normal examples. As we’ve already mentioned, we use only explosion video for our research. We assume that explosion can be considered a change in distribution, while other types are point anomalies. Given the small amount of data, we randomly chose a clip (a subsequence of whole frames’ sequences) from an abnormal subset for our research so that the explosion moment fell into the clip. For the normal subset, we pick clips randomly. Then, we generate sequences with length 16 by sampling each 4th frame from these clips. The dataset was manually divided into training and validation sets, keeping the proportion of abnormal videos equal to 0.25. The examples from the received data are shown in Figure 8.

**OOPS.** OOPS dataset includes 20338 fail compilation videos of different lengths. Each video consists of two parts: an intentional action before the fail (point of change) and an unintentional one after it [5]. To speed up experiments, we randomly pick 1000 videos for training after dropping videos without change points and 500 videos for the validation data. Following the preprocessing provided by the authors, we generate non-overlapping clips with 16 frames and FPS 8. In addition, we drop clips that completely lie after the change’s moment since they do not correspond to our task. The share of videos with change point in the training set is 0.43, and the validation set is 0.34. You can see examples of clips in Figure 9.

Table 2: Statistics for datasets used in our experiments.

Dataset	Single sample shape	Dataset size	Test size	% of sequences with changes	Sequence length
1D Normal	$1 \times 1$	1000	100	50	128
100D Normal	$100 \times 1$	1000	100	100	128
Human Activity	$561 \times 1$	319	32	100	20
Seq.MNIST	$28 \times 28 \times 1$	800	200	50	64
Explosion	$320 \times 240 \times 3$	200	88	25	16
OOPS	$112 \times 112 \times 3$	1574	887	39	16

### A.3 Implementation details

Here we provide details on architectures and training for used datasets.

**Synthetic datasets.** We use a GRU block with a hidden size of 8 and dropout 0.1 followed by the output linear layer with sigmoid activation for experiments with synthetic datasets. The number of GRU layers equals 1 in the case of 1D and 2 for 100D. We trained these networks for 25 epochs for

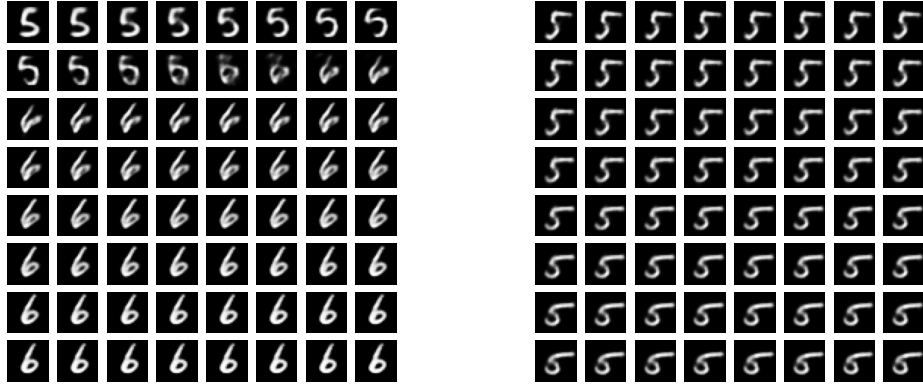


Figure 7: Example of MNIST sequences with (left) and without (right) change point.

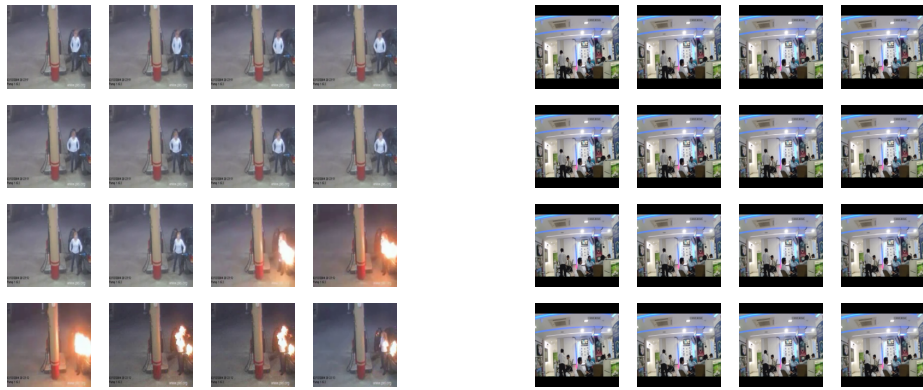


Figure 8: Example from Explosion data with (left) and without (right) change point correspondingly.



Figure 9: Example from OOPS data with (left) and without (right) change point correspondingly.

BCE and Custom losses and on 50 epochs for Combined loss (epochs were equally distributed for BCE and Custom losses).

**Human Activity dataset.** We conduct our experiments with the Human Activity dataset using a model consisting of a GRU block with 2 recurrent layers of 8 hidden dimensions and 0.1 dropout. This block is followed by a fully connected linear layer with the output size of 4, dropout 0.1, ReLU activation and output linear layer with the sigmoid. The number of training epochs was set up to 60

in the case of Custom and BCE loss functions and to 120 for the combined case (epochs were equally distributed for BCE and Custom losses).

**Sequences of MNIST images.** For MNIST images, we use 2 layers GRU with hidden size 100 and dropout 0.5 followed by linear layers with output size 50, dropout 0.5, ReLU activation and output layer with sigmoid activation functions. The number of training epochs was 60 for all experiments. They were distributed equally for two losses for Combined approach.

**Video datasets.** The architecture used in our experiments for video datasets consists of a CNN block and GRU block. The CNN block includes all pre-trained features from MobileNetV2 [20] followed by the linear layer. For the Explosion dataset, we use 100 output neurons in the CNN block, hidden size 50 for GRU and dropout 0.1. For the OOPS dataset, we use 512 as CNN’s output size, 128 hidden size for GRU and dropout 0.1. We use output linear layer with a dropout 0.25 and sigmoid activation functions for both of them. While training with proposed loss and BCE loss, we use Early Stopping criteria for validation loss with patience 10. For Combined loss, we use a fixed number of epochs for the first part with BCE loss and Early Stopping for training with the second our loss. For the Explosion dataset, the first step took 20 epochs and 10 for the OOPS dataset.

For all experiments, we use the Adam optimizer with learning rate  $1e-3$ .

#### **A.4 Extended version of results**

Extended values of metrics are provided in Table 3.



Table 3: Main quality metrics for considered loss functions.  $\uparrow$  marks metrics we want to maximize,  $\downarrow$  marks metrics we want to minimize.

Loss	Mean Time to FP	Mean delay $\downarrow$	TP $\uparrow$	FP $\downarrow$	Precision $\uparrow$	Recall $\uparrow$	F1 score $\uparrow$	Area under detec. curve $\downarrow$
Normal Distribution 1d								
BCE	95	0.040	43	4	0.960	<b>1.000</b>	0.956	1017.94
	99	1.380	44	<b>0</b>	0.980	0.957	0.978	
Custom (ours)	95	<b>0.010</b>	<b>45</b>	6	0.940	<b>1.000</b>	0.938	980.03
	99	1.080	44	<b>0</b>	0.980	0.957	0.978	
Combined (ours)	95	0.080	<b>45</b>	11	0.804	<b>1.000</b>	0.891	<b>978.12</b>
	99	0.840	<b>45</b>	<b>0</b>	<b>1.000</b>	0.978	<b>0.989</b>	
Multivariate Normal Distribution 100d								
BCE	60	<b>0.010</b>	<b>93</b>	7	<b>0.930</b>	<b>1.000</b>	<b>0.964</b>	2750.91
	75	30.470	87	<b>0</b>	<b>1.000</b>	0.870	0.930	
Custom (ours)	60	3.660	59	35	0.628	0.908	0.742	<b>2121.80</b>
	75	10.590	84	<b>0</b>	<b>1.000</b>	0.840	0.913	
Combined (ours)	60	0.930	92	7	0.929	0.989	0.958	2607.56
	75	14.610	83	<b>0</b>	0.830	0.830	0.907	
Human Activity								
BCE	10	1.438	19	13	0.594	<b>1.000</b>	0.745	69.32
	11	3.594	<b>26</b>	<b>4</b>	<b>0.867</b>	0.929	<b>0.897</b>	
Custom (ours)	10	<b>0.406</b>	7	25	0.219	<b>1.000</b>	0.359	59.06
	11	0.594	10	22	0.313	<b>1.000</b>	0.476	
Combined (ours)	10	0.688	15	17	0.469	<b>1.000</b>	0.638	<b>55.36</b>
	11	0.906	15	17	0.469	<b>1.000</b>	0.638	
MNIST								
BCE	44	0.938	60	37	0.619	<b>1.000</b>	0.534	477.40
	48	35.167	20	<b>0</b>	<b>1.000</b>	0.208	0.345	
Custom (ours)	44	1.115	35	61	0.365	<b>1.000</b>	0.534	<b>392.01</b>
	48	9.021	40	33	0.548	0.635	0.588	
Combined (ours)	44	<b>0.729</b>	50	48	0.510	<b>1.000</b>	0.676	516.84
	48	20.583	<b>74</b>	<b>0</b>	<b>1.000</b>	0.771	<b>0.871</b>	
Explosion								
BCE	13	0.670	8	11	0.421	0.533	0.471	5.40
	15	0.989	8	4	0.667	0.444	0.533	
Custom (ours)	13	<b>0.352</b>	8	21	0.276	0.571	0.372	4.35
	15	1.193	9	2	0.818	0.450	<b>0.581</b>	
Combined (ours)	13	0.625	<b>10</b>	18	0.357	<b>0.667</b>	0.465	<b>4.12</b>
	15	0.716	8	<b>1</b>	<b>0.889</b>	0.381	0.533	
OOPS								
BCE	6	<b>0.027</b>	5	<b>1</b>	0.833	0.006	0.011	20.23
	8	2.734	0	309	0.000	0.000	0.000	
Custom (ours)	6	0.352	118	2	0.983	0.134	0.236	15.02
	8	0.731	<b>153</b>	15	0.911	<b>0.182</b>	<b>0.303</b>	
Combined (ours)	6	0.036	45	<b>1</b>	<b>0.978</b>	0.051	0.097	<b>14.97</b>
	8	0.166	68	5	0.932	0.078	0.144	